

## Crystallization and preliminary X-ray diffraction studies of the influenza C virus glycoprotein

P. B. ROSENTHAL,<sup>a,b</sup> F. FORMANOWSKI,<sup>c†</sup> A. C. TREHARNE,<sup>a‡</sup> J. NEWMAN,<sup>a§</sup> J. J. SKEHEL,<sup>d</sup> H. MEIER-EWERT<sup>c</sup> AND D. C. WILEY<sup>a</sup> at <sup>a</sup>Department of Molecular and Cellular Biology, and Howard Hughes Medical Institute, and <sup>b</sup>Committee on Higher Degrees in Biophysics, Harvard University, Cambridge, Massachusetts, USA, <sup>c</sup>Abteilung für Virologie, Institut für Medizinische Mikrobiologie und Hygiene der Technischen Universität, München, Germany, and <sup>d</sup>National Institute for Medical Research, Mill Hill, London, England.

(Received 14 November 1995; accepted 17 April 1996)

### Abstract

Influenza C virus contains a single surface glycoprotein in its lipid envelope which is the hemagglutinin–esterase–fusion glycoprotein (HEF). HEF binds cell-surface receptors, is a receptor-destroying enzyme (a 9-*O*-acetylsterase), and mediates the fusion of virus and host cell membranes. A bromelain-released soluble form of HEF has been crystallized. Two different tetragonal forms have been identified from crystals with the same morphology [ $P4_{1(3)}22$ ,  $a = b = 154.5$ ,  $c = 414.4$  Å, and  $P4_{1(3)}2_12$ ,  $a = b = 217.4$ ,  $c = 421.4$  Å]. Both crystal forms share a common packing scheme. Synchrotron data collection and flash cooling of crystals have been used for high-resolution data collection.

### 1. Introduction

Influenza C is a lipid-enveloped orthomyxovirus and is a cause of disease in humans. Unlike influenza A and B which contain two surface glycoproteins, the hemagglutinin (HA) and the neuraminidase (NA), influenza C contains a single membrane glycoprotein which performs several functions critical to viral infection. The protein contains a binding site specific for cell-surface receptors containing *N*-acetyl-9-*O*-acetylneuraminic acid. A distinct enzyme active site functions as a receptor-destroying 9-*O*-acetylsterase. The glycoprotein also mediates the fusion of the virus and host membranes at the low pH encountered in endosomes, enabling the virus genome to enter the cytoplasm. The glycoprotein is thus a hemagglutinin–esterase–fusion factor (HEF) (Formanowski, Wharton, Calder, Hofbauer & Meier-Ewert, 1990; Herrler & Klenk, 1991; Herrler, Dürkop, Becht & Klenk, 1988).

Influenza C virus can be distinguished electron microscopically from influenza A and B by the presence of an hexagonal array of glycoprotein on the virus membrane. Image reconstructions from electron micrographs of negative-stained virions at 30 Å resolution suggest these arrays are formed by trimeric glycoproteins similar in size and shape to the influenza A HA (Hewatt, Cusack, Ruigrok & Verwey, 1984). HEF is a trimer of the disulfide-linked polypeptides HEF<sub>1</sub> and HEF<sub>2</sub>, with a total of 24 potential *N*-linked glycosylation sites. Like the HA, cleavage of HEF into the two glycopolypeptides, HEF<sub>1</sub> (65 kDa, 432 residues) and HEF<sub>2</sub> (30 kDa, 209 residues), is required for the membrane-fusion activity of the molecule (Herrler, Compans & Meier-

Ewert, 1979; Ohuchi, Ohuchi & Mifune, 1982; Kitame, Sugawara, Ohwada & Homma, 1982; Formanowski *et al.*, 1990). However, HEF has less than 15% sequence identity to the HA (Nakada, Creager, Krystal, Aaronson & Palese, 1984; Pfeifer & Compans, 1984). HEF<sub>1</sub> is 104 amino acids longer than influenza A HA<sub>1</sub>. It contains the enzyme active site, serine 71 has been identified as the catalytic active-site serine, and the nature of the flanking residues suggests that the protein defines a new class of serine esterases (Herrler, Multhaup, Beyreuther & Klenk, 1988; Vlasak, Muster, Lauro, Powers & Palese, 1989; Hayes & Varki, 1989). HEF<sub>2</sub> is similar in length to influenza A HA<sub>2</sub> and contains the C-terminal transmembrane anchor which we have removed by bromelain digestion (see below). The N-terminal hydrophobic fusion peptide of HEF<sub>2</sub> is unusual among fusion peptides found in enveloped viruses in containing two aspartic acids at residues 5 and 6 (Nakada *et al.*, 1984; Pfeifer & Compans, 1984). The time course of influenza C virus membrane fusion shows a kinetic lag which suggests that it may be possible to observe intermediate steps in the HEF-mediated fusion mechanism. (Formanowski *et al.*, 1990).

X-ray structures of the HA (Wilson, Skehel & Wiley, 1981) and NA (Varghese, Laver & Colman, 1983; Burmeister, Ruigrok & Cusack, 1991) have greatly increased our understanding of the molecular basis of viral infection and are being used to design antiviral agents (von Itzstein *et al.*, 1993; Watowich, Skehel & Wiley, 1994; Glick, Toogood, Wiley, Skehel & Knowles, 1991; Spaltenstein & Whitesides, 1991; Toogood, Galliker, Glick & Knowles, 1991; Luo *et al.*, 1995; White *et al.*, 1995; Bodian *et al.*, 1993). Crystallographic studies at atomic resolution are required to understand the multiple functions of HEF and the evolutionary relationship of influenza C to other members of the orthomyxovirus and paramyxovirus families. In addition, HEF<sub>1</sub> has 30% sequence identity to the hemagglutinin-esterase (HE) found on the surface of some coronaviruses, which express a 65 kDa protein lacking an HEF<sub>2</sub> homologue (Luytjes, Bredenbeek, Noten, Horzinek & Spaan, 1988; Vlasak, Luytjes, Leider, Spaan & Palese, 1988; King, Potts & Brian, 1985).

This report describes the crystallization of a bromelain-released soluble fragment of influenza C HEF (bHEF). Bromelain digestion results in the removal of the residues beyond 175 or 176 of HEF<sub>2</sub> producing a trimeric molecule lacking only the 4 kDa C-terminal peptide containing the hydrophobic transmembrane and cytoplasmic segments for each monomer (Formanowski & Meier-Ewert, 1988, 1990). The crystals are suitable for high-resolution crystallographic studies. Preliminary analysis of the diffraction data is presented.

† Current address: Cressier, Switzerland. ‡ Current address: Crystallography Research Program, Oklahoma Medical Research Foundation, Oklahoma City, OK, USA. § Current address: Department of Biochemistry and Molecular Biophysics, Columbia University, New York, NY, USA.

## 2. Methods

### 2.1. Purification

C/Johannesburg/1/66 virions were grown in MDCK type I cells as previously described (Formanowski & Meier-Ewert, 1988). The glycoprotein was isolated using the conditions described by Formanowski & Meier-Ewert (Formanowski & Meier-Ewert, 1988) with some modifications. Virus was suspended at  $2 \text{ mg ml}^{-1}$  in buffer *A* ( $50 \text{ mM Tris-HCl pH 8.0}$ ,  $100 \text{ mM NaCl}$ ,  $10 \text{ mM CaCl}_2$ ,  $0.1\% \text{ NaN}_3$ ). Bromelain digestion was accomplished by adding 2-mercaptoethanol to  $0.05 \text{ M}$ , bromelain (Sigma) to  $0.5 \text{ mg}$  per  $\text{mg}$  of virus, and incubating at  $306 \text{ K}$  for  $18 \text{ h}$ . Digested virus was then pelleted at  $100\,000g$  for  $1 \text{ h}$ . Supernatant was placed in a centrifuge  $100$  (Amicon,  $100 \text{ kDa}$  MW cutoff) and the volume reduced to  $1/10$  and then diluted with buffer *B* ( $10 \text{ mM Tris-HCl pH 7.4}$ ,  $140 \text{ mM NaCl}$ ,  $10 \text{ mM CaCl}_2$ ,  $0.1\% \text{ NaN}_3$ ). The dilution and concentration steps were repeated several times until bromelain (MW  $33 \text{ kDa}$ ) had passed through the membrane and only bHEF was retained in the concentrate. The volume was further reduced until the bHEF concentration was at least  $10 \text{ mg ml}^{-1}$ . In some cases the protease inhibitor E64 was used to stop bromelain activity.

### 2.2. Crystallization

Concentrated bHEF was crystallized by vapor diffusion in 24-well trays (Linbro). Hanging drops were composed of  $2 \mu\text{l}$  bHEF ( $10\text{--}20 \text{ mg ml}^{-1}$ ) in buffer *B* and  $2 \mu\text{l}$  well solution.

Crystals grew from well solutions containing  $56\text{--}60\%$  saturated ammonium sulfate,  $10 \text{ mM Tris-HCl pH 7.4}$ ,  $140 \text{ mM NaCl}$ ,  $10 \text{ mM CaCl}_2$ , and  $0.1\% \text{ NaN}_3$ . Crystals were harvested into a well solution containing  $60\%$  ammonium sulfate.

Crystals of identical morphology were grown by the same method using  $1.32 \text{ M}$  sodium citrate  $\text{pH 6.5}$ ,  $0.1\% \text{ NaN}_3$  as the well solution and harvested into  $1.35 \text{ M}$  sodium citrate  $\text{pH 6.5}$ .

Sodium dodecyl sulfate polyacrylamide electrophoresis (SDS-PAGE, Laemmli, 1970) was performed on washed, dissolved crystals. Washed, dissolved crystals were tested for 9-*O*-acetyl esterase activity by detecting the release of acetic acid from 9-*O*-acetyl Neu5Ac (a gift from John Hanson) using an acetic acid detection assay (Boehringer-Mannheim) or by spectrophotometric assay of hydrolysis of the substrate *p*-nitrophenylacetate (Vlasak, Krystal, Nacht & Palese, 1987; Vlasak *et al.*, 1989).

### 2.3. X-ray crystallography

Crystals were mounted in washed glass capillaries for data collection at room temperature. Precession photographs were taken on a Supper precession camera at a crystal-to-film distance of  $10 \text{ cm}$  using Reflex-25 film (CEA).  $\text{Cu K}\alpha$  X-rays were generated by an Elliot GX-6 rotating anode with a  $100 \mu\text{m}$  focus cup and Franks-type focusing mirrors (Harrison, 1968) and a  $150 \mu\text{m}$  pinhole.

Crystals were prepared for cryocrystallography by addition of glycerol to the harvest solution as a cryoprotectant. Ammonium sulfate harvest solution was made up to  $5\text{--}25\%$  glycerol in  $5\%$  steps. Sodium citrate harvest solution was made up to  $3\text{--}12\%$  glycerol in  $3\%$  steps. Crystals were transferred in steps ( $5 \text{ min}$ ) through increasing glycerol concentrations and then placed on silanized coverslips. The crystals were picked up with a wire or rayon loop (Teng,

1990) mounted on a magnetic cap (Rodgers, 1994), and flash cooled on the camera spindle at  $108 \text{ K}$  in a gaseous nitrogen stream. The cryogenic apparatus used was either a Max cryostat (Hope *et al.*, 1989) or a Molecular Structure Corporation Low-Temperature System.

Data collection was performed at the Cornell High Energy Synchrotron Source F1 beamline ( $\lambda = 0.91 \text{ \AA}$ ) using Fuji image plates, a  $150 \mu\text{m}$  collimator, and a crystal-to-plate distance of  $35 \text{ cm}$ . Silicon powder rings or ice rings were used to measure the plate distance.  $1^\circ$  oscillation photographs were recorded with a typical exposure of  $2 \text{ min}$ . Image plates were scanned using either a Fuji BAS2000 scanner or a Kodak scanner. X-ray data were indexed and integrated using DENZO (Otwinowski, 1991) and further analyzed with either SCALEPACK (Otwinowski, 1991) or with programs from the CCP4 suite (Collaborative Computational Project, Number 4, 1994).

## 3. Results and discussion

bHEF crystals grew in one to two weeks as shown in Fig. 1 and were typically cubes  $0.15\text{--}0.2 \text{ mm}$  on a side or were slightly elongated in one dimension. SDS-PAGE demonstrated that the crystals contained the expected disulfide-linked polypeptides HEF<sub>1</sub> and HEF<sub>2</sub>. Protein dissolved from washed crystals possessed 9-*O*-acetyl esterase activity.

Space-group determination was initially made at low resolution by precession photography at room temperature. Examination of  $2^\circ$  screenless precession photos of layers  $0kl$ ,  $h0l$  and  $hk0$  led to the assignment of both the ammonium sulfate and sodium citrate crystal forms to space group  $P4_122$  or its enantiomorph  $P4_322$  with  $a = b = 155$ ,  $c = 415 \text{ \AA}$ ,  $\alpha = \beta = \gamma = 90^\circ$ . The  $a$ ,  $b$  and  $c$  axes are normal to the faces of the crystal. Crystals showed well ordered diffraction patterns to  $3.5 \text{ \AA}$  with mosaicity of  $0.15^\circ$  full-width. Radiation sensitivity of the crystals prevented collection of more than  $\frac{1}{2}^\circ$  of oscillation data per crystal, and the crystals diffracted to high resolution for less than  $120 \text{ s}$  in the CHESS F1 beam.

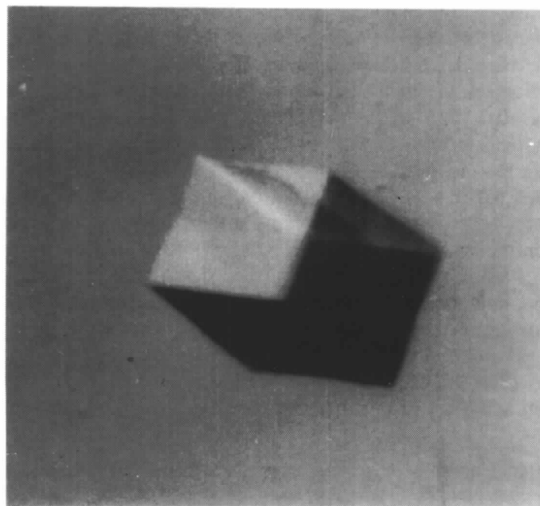


Fig. 1. A crystal of bHEF grown from sodium citrate. Each dimension is approximately  $0.2 \text{ mm}$ .

Table 1. Summary of diffraction data

Crystal form	I	II
Precipitant	Ammonium sulfate	Sodium citrate
Space group	$P4_122$ or $P4_322$	$P4_12_12$ or $P4_32_12$
Unit cell (Å)	$a = b = 154.5$ , $c = 414.4$	$a = b = 217.4$ , $c = 421.4$
$R_{\text{sym}} * \dagger$ (%)	8.2	4.5
Unique reflections <sup>†</sup>	42354	82985
Completeness <sup>†</sup> (%)	99	99

$$* R_{\text{sym}} = \sum (|I - \bar{I}|) / \sum \bar{I}. \quad \dagger \text{Data to } 4 \text{ \AA}.$$

Subsequent data collection was performed at CHESS on the F1 beamline using flash cooling of the crystals. Complete data sets were collected from single crystals before significant radiation damage was observed. 150  $\mu\text{m}$  collimation and a plate distance of 35 cm at  $\lambda = 0.91 \text{ \AA}$  were sufficient to resolve the diffraction spacings associated with

the long 414  $\text{\AA}$   $c$  axis. The ammonium sulfate crystal form showed similar cell dimensions under the conditions described for cryocrystallography as at room temperature, but an increase of mosaicity to 0.5° full-width. Diffraction has been observed to 2.4  $\text{\AA}$  resolution. Statistics on complete data sets from these crystals, called form I, are reported in Table 1.  $R_{\text{sym}}$  for reflections related by individual mirror planes and examination of systematic absences confirmed the original space-group assignment as  $P4_122$  or  $P4_322$ .

The sodium citrate crystal form, when observed under the conditions described for cryocrystallography, diffracted to 2.8  $\text{\AA}$  with mosaicity 0.25°, but showed a different space group than determined for crystals of identical morphology at room temperature. The data were indexed as  $a = b = 217.4$ ,  $c = 421.4 \text{ \AA}$ ,  $\alpha = \beta = \gamma = 90^\circ$  with the  $c$  axis normal to one face and the  $a$  and  $b$  axes now 45° from the normal on the remaining faces. Examination of pseudoprecession photo-

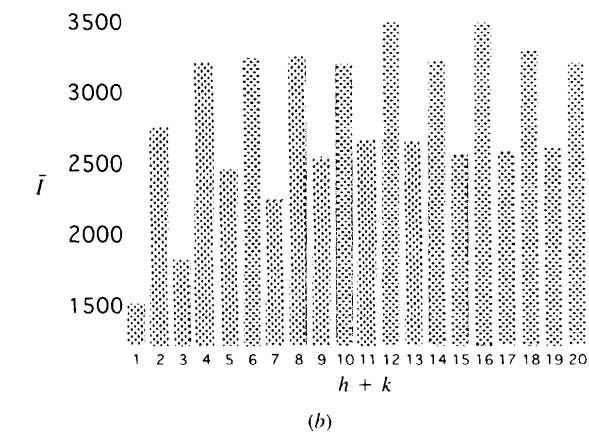
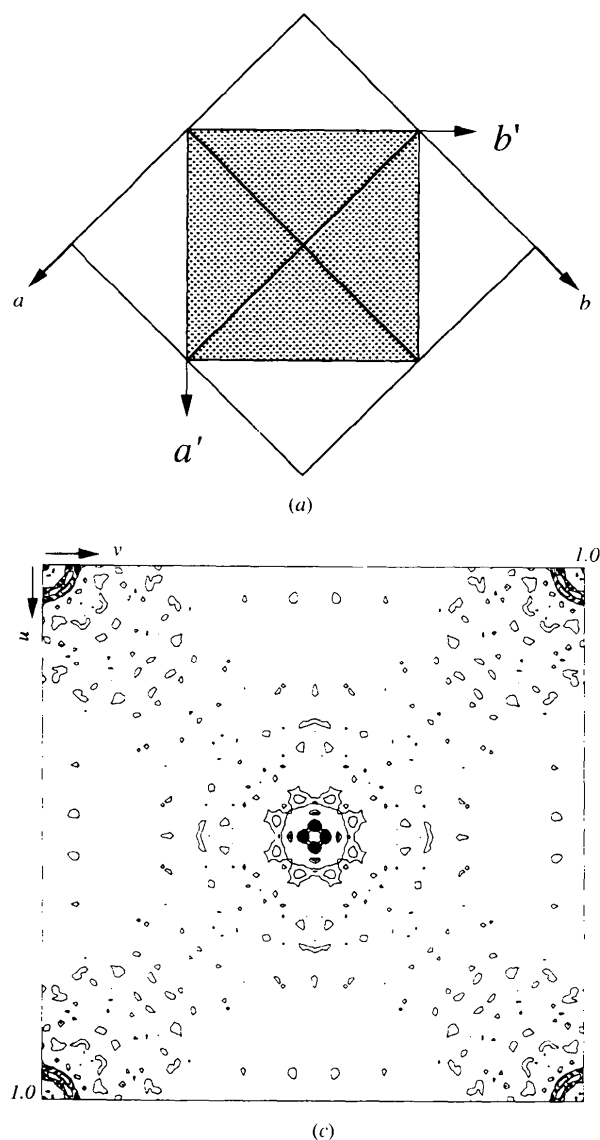


Fig. 2. Relationship between form I and form II crystals. (a) The diagram shows a comparison of the unit-cell axes of both crystal forms as viewed down their common  $c$  axis. Form I  $P4_122$ : four unit cells are represented as four squares with edges parallel to the  $a$  and  $b$  axes. Form II  $P4_12_12$ : a single unit cell is represented by a shaded square with edges parallel to the  $a'$  and  $b'$  axes. The 217  $\text{\AA}$  axes of form II, are approximately the same length as the  $ab$  diagonals of form I. A unit cell of the form II lattice has twice the volume of the form I unit cell and is rotated by 45°. (b) Analysis of diffraction data from form II crystals. Average intensity is plotted for the reciprocal-space planes  $h+k = n$ . Intensity is greater for  $h+k$  even, evidence for pseudo- $C$ -centering. (c)  $U, V, W = 1.6 \text{ \AA}$  section of the form II native Patterson map. A section from  $U = 0$  to 1.0,  $V = 0$  to 1.0 (entire unit cell) is shown. Pseudo- $C$ -centering is indicated by peaks near  $U = V = \frac{1}{2}$ . Contours are drawn at 0.5RMS density of the map starting at 0.5RMS. The large non-origin peaks in each asymmetric unit are interpreted as translation vectors of approximately  $(\frac{1}{2}, \frac{1}{2}, 0)$  between non-crystallographically related molecules lying in similar orientations.

graphs generated from three-dimensional data,  $R_{\text{sym}}$  for reflections related by individual mirror planes, and systematic absences indicated the space group is  $P4_12_12$  or  $P4_32_12$ . Data-collection statistics on these crystals, called form II, are given in Table 1.

Though form II crystals have twice the unit-cell volume of form I crystals, both cells possess a common packing scheme. Both forms are tetragonal with similar length  $c$  axes, and the 217 Å  $a$  axis of form II crystals is the length of the  $ab$  diagonal of form I crystals. Fig. 2(a) shows how the two lattices can be superimposed when rotated 45° with respect to each other about their common  $c$  axis. Such a rotation is also consistent with the location of the symmetry elements of each form with respect to the single observed crystal morphology. A cross rotation function (Crowther, 1972) between the two forms identifies a single  $10.6\sigma$  peak for a relative rotation of 45° about the  $c$  axis, suggesting that molecular contents of form I and form II are similar when related by this rotation.

The addition of  $C$ -centering translations to the general positions of a  $P4_12_12$  lattice (form II) produces a  $C$ -centered lattice which is equivalent to a  $P4_122$  lattice (form I) with unit cells that are half volume and rotated by 45°, as shown in Fig. 2(a). Examination of the diffraction data and the native Patterson function suggests that form II is pseudo- $C$ -centered. In Fig. 2(b), a plot of average  $I$  for reciprocal-space planes  $h+k=n$  is given. Reduced intensity for  $h+k$  odd is evidence for pseudo- $C$ -centering. The native Patterson function calculated for form II shows a large peak near  $U = \frac{1}{2}$ ,  $V = \frac{1}{2}$ ,  $W = 0$  as shown in Fig. 2(c). This peak is interpreted as a translation vector  $(\frac{1}{2}, \frac{1}{2}, 0)$  between non-crystallographic symmetry-related molecules within the asymmetric unit lying in similar orientations. If the  $C$ -centering were exact, form II would be identical to form I, and the molecules related by the non-crystallographic translation vector would be related by a crystallographic symmetry operation. Similar observations of common packing schemes in  $P4_122$  and  $P4_12_12$  have been reported for the complement proteins C3 and C3b (Sørensen *et al.*, 1994).

Structure determination of bHEF is now in progress using both crystal forms described here. These efforts include isomorphous replacement and molecular replacement using the influenza A hemagglutinin (Wilson *et al.*, 1981) as a source of phases. Both crystal forms have the potential for non-crystallographic symmetry averaging around the molecular threefold axis (Bricogne, 1976). Crystallographic studies of influenza C ligand binding have also been initiated with X-ray data collected from crystals soaked with the receptor analogue and 9-*O*-acetylcysteine inhibitor 9-acetamido Neu5Ac $\alpha$ 2Me. (Herrler *et al.*, 1992; Hanson & Rosenthal, 1990).

We thank Mia Frayser for excellent technical assistance, members of the Harrison-Wiley laboratory and the staff of the Cornell High Energy Synchrotron Source for assistance with data collection, and John Hanson for providing the 9-*O*-acetyl Neu5Ac. This research was supported by the National Institutes of Health (AI13654), The Deutsche Forschungsgemeinschaft, and the Medical Research Council (UK). DCW is an Investigator of the Howard Hughes Medical Institute.

## References

- Bodian, D. L., Yamasaki, R. B., Buswell, R. L., Stearns, J. F., White, J. M. & Kuntz, I. D. (1993). *Biochemistry*, **32**, 2967–2978.
- Bricogne, G. (1976). *Acta Cryst.* **A32**, 832–847.
- Burmeister, W. P., Ruigrok, R. W. H. & Cusack, S. (1991). *EMBO J.* **11**, 49–56.
- Collaborative Computational Project, Number 4 (1994). *Acta Cryst.* **D50**, 760–763.
- Crowther, R. A. (1972). In *The Molecular Replacement Method*, edited by M. G. Rossmann. New York: Gordon & Breach.
- Formanowski, F. & Meier-Ewert, H. (1988). *Virus Res.* **10**, 177–192.
- Formanowski, F. & Meier-Ewert, H. (1990). Abstracts of the VIIIth International Congress of Virology, pp. 17–624, Abstract 218.
- Formanowski, F., Wharton, S. A., Calder, L. J., Hofbauer, C. & Meier-Ewert, H. (1990). *J. Gen. Virol.* **71**, 1181–1188.
- Glick, G. D., Toogood, P. L., Wiley, D. C., Skehel, J. J., Knowles, J. R. (1991). *J. Biol. Chem.* **266**, 23660–23669.
- Hanson, J. & Rosenthal, P. (1990). Unpublished results.
- Harrison, S. C. (1968). *J. Appl. Cryst.* **1**, 84–90.
- Hayes, B. & Varki, A. (1989). *J. Biol. Chem.* **264**(32), 19443–19448.
- Herrler, G., Compans, R. W. & Meier-Ewert, H. (1979). *Virology*, **99**, 49–56.
- Herrler, G., Dürkop, I., Becht, H. & Klenk, H.-D. (1988). *J. Gen. Virol.* **69**, 839–846.
- Herrler, G., Gross, H.-J., Imhof, A., Brossmer, R., Milks, G. & Paulson, J. C. (1992). *J. Biol. Chem.* **267**(18), 12501–12505.
- Herrler, G. & Klenk, H.-D. (1991). *Adv. Virus Res.* **40**, 213–234.
- Herrler, G., Multhaup, G., Beyreuther, K. & Klenk, H.-D. (1988). *Arch. Virol.* **102**, 269–274.
- Hewatt, E. A., Cusack, S., Ruigrok, R. W. H. & Verwey, C. (1984). *J. Mol. Biol.* **175**, 175–193.
- Hope, H., Frowlow, F., von Böhlen, K., Makowski, I., Kratky, C., Halfon, Y., Danz, H., Webster, P., Bartels, K., Wittmann, H. & Yonath, A. (1989). *Acta Cryst.* **B45**, 190–199.
- Itzstein, M., von Wu, W.-Y., Kok, G. B., Pegg, M. S., Dyason, J. C., Jin, B., Phan, T. V., Smythe, M. L., White, H. F., Oliver, S. W., Colman, P. M., Varghese, J. N., Ryan, D. M., Woods, J. M., Bethal, R. C., Hotham, V. J., Cameron, J. M. & Penn, C. R. (1993). *Nature (London)*, **336**, 418–423.
- King, B., Potts, B. J. & Brian, D. A. (1985). *Virus Res.* **2**, 53–59.
- Kitame, F., Sugawara, K., Ohwada, K. & Homma, M. (1982). *Arch. Virol.* **73**, 357–361.
- Laemmli, U. (1970). *Nature (London)*, **227**, 680–685.
- Luo, M., Jedrzejewski, M. J., Singh, S., White, C. L., Brouillette, W. J., Air, G. M. & Laver, W. G. (1995). *Acta Cryst.* **D51**, 504–510.
- Luytjes, W., Bredenbeek, P. J., Noten, A. F. H., Horzinek, M. C. & Spaan, W. J. M. (1988). *Virology*, **166**, 415–422.
- Nakada, S., Creager, R. S., Krystal, M., Aaronson, R. P. & Palese, P. (1984). *J. Virol.* **50**, 118–124.
- Ohuchi, M., Ohuchi, R. & Mifune, K. (1982). *J. Virol.* **42**, 1076–1079.
- Otwinowski, Z. (1991). *DENZO. A Film Processing Program for Macromolecular Crystallography*. Yale University, New Haven, CT, USA.
- Pfeifer, J. B. & Compans, R. (1984). *Virus Res.* **1**, 281–296.
- Rodgers, D. W. (1994). *Structure*, **2**, 1135–1140.
- Sørensen, A. H., Dolmer, K., Thirup, S., Andersen, G. R., Sottrup-Jensen, L. & Nyborg, J. (1994). *Acta Cryst.* **D50**, 786–789.
- Spaltenstein, A. & Whitesides, G. (1991). *J. Am. Chem. Soc.* **113**, 686–687.

- Teng, T.-Y. (1990). *J. Appl. Cryst.* **23**, 387-391.
- Toogood, P. L., Galliker, P. K., Glick, G. D. & Knowles, J. R. (1991). *J. Med. Chem.* **34**(10), 3138-3140.
- Varghese, J. N., Laver, W. G. & Colman, P. M. (1983). *Nature (London)*, **303**, 35-40.
- Vlasak, R., Krystal, M., Nacht, M. & Palese, P. (1987). *Virology*, **160**, 419-425.
- Vlasak, R., Luytjes, W., Leider, J., Spaan, W. & Palese, P. (1988). *J. Virol.* **62**, 4686-4690.
- Vlasak, R., Muster, T., Lauro, A. M., Powers, J. C. & Palese, P. (1989). *J. Virol.* **63**(5), 2056-2062.
- Watowich, S., Skehel, J. J. & Wiley, D. C. (1994). *Structure*, **2**(8), 719-731.
- White, C. L., Janakiraman, M. N., Laver, W. G., Philippon, C., Vasella, A., Air, G. M. & Luo, M. (1995). *J. Mol. Biol.* **245**, 623-634.
- Wilson, I. A., Skehel, J. J. & Wiley, D. C. (1981). *Nature (London)*, **289**, 366-373.